

Crystal and Molecular Structure, Spectroscopic Properties, and Electrophilic Reactivity of Sodium Pentacyanonitrosylmate(II) Dihydrate

Luis M. Baraldo,[†] Marcela S. Bessega,[†] Graciela E. Rigotti,[‡] and José A. Olabe^{*†}

Departamento de Química Inorgánica, Analítica y Química Física, INQUIMAE, Facultad de Ciencias Exactas y Naturales, Universidad de Buenos Aires, 1428 Capital Federal, República Argentina, and Laboratorio de Cristalografía, PROFIMO, Departamento de Física, Facultad de Ciencias Exactas, Universidad Nacional de La Plata, 1900 La Plata, República Argentina

Received May 18, 1994[⊗]

Sodium pentacyanonitrosylmate(II) dihydrate, $\text{Na}_2[\text{Os}(\text{CN})_5\text{NO}] \cdot 2\text{H}_2\text{O}$, was synthesized by photolyzing a mixture of hexacyanoosmate(II) and nitrite ion, with further purification through ion-exchange and precipitation techniques. The compound is isostructural with the iron and ruthenium analogue species. The crystals are orthorhombic (*Pnmm*) with $a = 6.312$ (1) Å, $b = 12.090$ (2) Å, $c = 15.828$ (3) Å, and $Z = 4$. Relevant lengths and angles within the distorted anion octahedra are compared for the three (Fe, Ru, Os) compounds. IR and UV–visible spectral data are also comparatively discussed. The results are indicative of a very strong σ -, as well as back-bonding π -interaction from Os toward nitrosyl and cyanides. The complex is electrophilically reactive toward several bases such as OH^- , SH^- and N_2H_4 . With OH^- , an equilibrium reaction is established, $[\text{Os}(\text{CN})_5\text{NO}]^{2-} + 2\text{OH}^- \rightleftharpoons [\text{Os}(\text{CN})_5\text{NO}_2]^{4-} + \text{H}_2\text{O}$, with $K = 42 \pm 1 \text{ M}^{-2}$ ($I = 1 \text{ M}$, $25.0 \text{ }^\circ\text{C}$). From the kinetic and mechanistic analysis, $k_{\text{obs}} = 1.37 \times 10^{-4} \text{ M}^{-1} \text{ s}^{-1}$, is determined by the rate of nucleophilic attack of OH^- into $[\text{Os}(\text{CN})_5\text{NO}]^{2-}$ in the elementary step. Kinetic and equilibrium results are compared with those obtained for iron and ruthenium pentacyanonitrosyl analogues, as well as for other nitrosyl complexes containing ruthenium and osmium; thus, the different factors influencing nucleophilic rates and affinities are discussed, namely charge, radius and polarizability of the reactants, as well as the energy of the $\pi^*(\text{NO})$ level. The reactions of $[\text{Os}(\text{CN})_5\text{NO}]^{2-}$ with other nucleophiles proceed through initial adduct formation and further decomposition.

Introduction

The coordination chemistry of osmium has been extensively developed in recent years.¹ However, limited work is related to cyanide and mixed cyanide complexes,^{1–4} in contrast with the studies on the $[\text{Fe}(\text{CN})_5\text{L}]^{n-}$ and, more recently, the $[\text{Ru}(\text{CN})_5\text{L}]^{n-}$ ions.^{5–7} A varied amount of L ligands with different σ - and π -bonding capabilities have been used, allowing for systematic studies on substitution- and electron transfer-reactions.⁵ In view of the lack of appropriate series of d^6 , low-spin complexes containing all the members of group 8 as metal centers, it seemed worth making efforts to prepare the osmium analogue series.

A potassium salt of the $[\text{Os}(\text{CN})_5\text{NO}]^{2-}$ ion was obtained many years ago and IR and UV–visible spectral results were

reported.⁸ But these studies are of restricted value, because no structural data are available and, strikingly, the compound proved to be insoluble in water.⁹

We report on the molecular and electronic structure of the nitrosyl derivative, after synthesizing single crystals of the very soluble sodium salt. The properties of the new compound are interesting in their own right, in the context of a general concern on the structure¹⁰ and chemistry^{11,12} of coordinated nitrosyl, and allow for useful comparisons with the bonding properties of the iron and ruthenium pentacyanonitrosyl analogues.

The electrophilic reactions of coordinated nitrosyl are of particular interest in the field of biochemistry, in view of the hypotensive action of the nitroprusside ion,¹³ as well as other implications of NO in a number of diverse physiological process.¹⁴ Thus, we report also a kinetic and mechanistic analysis of the reaction of $[\text{Os}(\text{CN})_5\text{NO}]^{2-}$ with OH^- , as well as a preliminary exploration of the addition reactions with other nucleophiles, SH^- and N_2H_4 . Besides, the electrophilic reactions of $[\text{Os}(\text{CN})_5\text{NO}]^{2-}$ proved to be successful in the synthetic efforts to prepare a new series of $[\text{Os}(\text{CN})_5\text{L}]^{n-}$ complexes.¹⁵

Experimental Section

Synthesis of $\text{Na}_2[\text{Os}(\text{CN})_5\text{NO}] \cdot 2\text{H}_2\text{O}$. Sodium nitrite (4 mmol, Mallinckrodt) was added to a millimolar aqueous solution (80 mL) of

* To whom correspondence should be addressed. FAX: 54-1-7820441. E-mail: olabe@inorba.uba.ar.

[†] Universidad de Buenos Aires.

[‡] Universidad Nacional de La Plata.

[⊗] Abstract published in *Advance ACS Abstracts*, November 1, 1994.

- (1) Lay, P. A.; Harman, W. D. *Adv. Inorg. Chem.* **1991**, *37*, 219.
- (2) Sharpe, A. G. *The Chemistry of Cyano Complexes of the Transition Metals*; Academic Press: New York, 1976; Chapter VII.
- (3) Griffith, W. P. *Comprehensive Coordination Chemistry*; Wilkinson, G., Gillard, R. D., Mc Cleverty, J. A., Eds.; Pergamon Press: Oxford, England, 1987; Vol. 4, Chapter 46, p 525.
- (4) (a) Constable, E. C.; Housecraft, C. E. *Coord. Chem. Rev.* **1990**, *124*, 183. (b) Ward, M. C. *Coord. Chem. Rev.* **1991**, *127*, 1.
- (5) Macartney, D. H. *Rev. Inorg. Chem.* **1988**, *9*, 101.
- (6) Olabe, J. A.; Gentil, L. A.; Rigotti, G.; Navaza, A. *Inorg. Chem.* **1984**, *23*, 4297.
- (7) (a) Johnson, C. R.; Shepherd, R. E. *Inorg. Chem.* **1983**, *22*, 1117. (b) Chevalier, A. A.; Gentil, L. A.; Olabe, J. A. *J. Chem. Soc., Dalton Trans.* **1991**, 1959. (c) Hoddenbagh, J. M. A.; Macartney, D. H. *Inorg. Chem.* **1986**, *25*, 380, 2099. (d) Almaraz, A. E.; Gentil, L. A.; Olabe, J. A. *J. Chem. Soc., Dalton Trans.* **1989**, 1973. (e) Tokman, A. L.; Gentil, L. A.; Olabe, J. A. *Polyhedron* **1989**, *8*, 2091. (f) Chevalier, A. A.; Gentil, L. A.; Olabe, J. A. *Polyhedron* **1992**, *11*, 1229.

(8) Baran, E. J.; Müller, A. Z. *Anorg. Chem.* **1969**, *370*, 283.

(9) In fact, concentrated reddish solutions containing $[\text{Os}(\text{CN})_5\text{NO}]^{2-}$ and K^+ ions could be handled by us without precipitation. We believe that the claimed $[\text{M}(\text{CN})_5\text{NO}]\text{K}_2 \cdot 2\text{H}_2\text{O}$ salts⁸ ($\text{M} = \text{Ru}, \text{Os}$) could be Prussian blue type compounds containing the $[\text{M}(\text{CN})_5\text{NO}]^{2-}$ anion.

(10) Feltham, R. D.; Enemark, J. H. *Top. Stereochem.* **1981**, *12*, 155.

(11) Mc Cleverty, J. A. *Chem. Rev.* **1979**, *79*, 53.

(12) Bottomley, F. In *Reactions of Coordinated Ligands*; Braterman, P. S., Ed.; Plenum: New York, 1989; Vol. 2, p 115.

(13) Butler, A. R.; Glidewell, C. *Chem. Soc. Rev.* **1987**, *16*, 361.

(14) Stamler, J. S.; Singel, D. J.; Loscalzo, J. *Science* **1992**, *258*, 1898.

(15) Slep, L. D.; Baraldo, L. M.; Olabe, J. A. Work in progress.

Table 1. Summary of Crystal Data and Intensity Data Collection for Na₂[Os(CN)₅NO]·2H₂O

chem formula: C ₅ H ₄ N ₆ Na ₂ O ₃ Os	fw = 432.3
a = 6.312(1) Å	space group = <i>Pnnm</i>
b = 12.090(2) Å	T = 22 °C
c = 15.828(3) Å	λ = 0.710 73 Å
V = 1207.9(6) Å ³	ρ(calcd) = 2.38 g cm ⁻³
Z = 4	μ = 102 cm ⁻¹
	R(F _o) ^a = 0.0237
	R _w (F _o) ^b = 0.0267

$${}^a R = \sum(|F_o| - |F_c|)/\sum|F_o|, {}^b R_w = \sum w^{1/2}(|F_o| - |F_c|)/\sum w^{1/2}|F_o|.$$

K₄[Os(CN)₆] (prepared by following the procedure for K₄[Ru(CN)₆]¹⁶ but starting from OsO₄ (Johnson Matthey). The pH was adjusted to 4.0 with acetic acid. The mixture was irradiated in a quartz vessel (100 mL) with two low-pressure Hg lamps for 30 h. Then it was evaporated to dryness, redissolved in deionized water (10 mL), and methanol was added to induce the precipitation of excess potassium hexacyanoosmate. The filtered solution was concentrated to 3–4 mL and loaded into a Sephadex G-25 column (ca. 4 × 150 cm) in order to separate monomers from dimers; no detailed work was undertaken to characterize properly the latter species, although the spectral evidences suggest that cyanide-bridged complexes of mixed-valence type are formed. A further purification was obtained by loading onto an ionic exchange bed (QAE-25) and eluting with a solution of KNO₃ (0.5–1 M). A solution of AgNO₃ (in HNO₃) was added to the eluate and a yellow precipitate was obtained; it was filtered off and washed with water several times. The silver salt precipitate was mixed with an aqueous solution of NaI, in a slight deficiency. The resulting precipitate (AgI) was separated by filtering with a nitrocellulose membrane (pore diameter 0.05) and the solution was evaporated to dryness. From the solid yellow mass (yield > 60%), single crystals could be picked for the crystallographic study. Analytical data for C, H, N were obtained with a Carlo Erba Ea 1108 elemental analyzer; sodium was measured by emission photometry. Anal. Calcd for C₅H₄N₆Na₂O₃Os: C, 13.89; H, 0.93; N, 19.44; Na, 10.60. Found: C, 13.31; H, 0.88; N, 19.10; Na, 10.00.

Spectral Measurements. The IR spectrum was recorded on a FTIR Nicolet 510P spectrophotometer, in KBr pellets. Electronic absorption spectra and kinetic experiments were performed on a Hewlett Packard 8452A diode array instrument.

Crystallographic Analysis. A yellow prismatic single crystal (0.3 × 0.2 × 0.1 mm) was mounted on an Enraf-Nonius CAD-4 four-circle diffractometer, employing graphite-monochromated Mo Kα radiation. It was used for the determination of accurate unit cell parameters and collection of intensity data (θ - 2θ collection method). The cell parameters and orientation matrix were determined by least squares from the setting angles of 20 reflections having 30° < 2θ < 34°. Intensity data were corrected for Lorentz, polarization and absorption effects (DIFABS, MolEN, ENRAF-NONIUS 1990, μ = 102 cm⁻¹). Other crystal data and data collection and refinement parameters are given in Table 1. The numbers of total and independent reflections measured were 2048 and 1560, respectively; R_{int} = 0.0074, θ_{max} = 30°.

The structure was solved by combination of Patterson and difference Fourier methods¹⁷ and refined by the method of full-matrix least-squares and F magnitudes,¹⁸ with about 13 data independent parameters. Hydrogen atoms were not found. R values are shown in Table 1. Agreement factor was S = 1.63, (Δ/σ)_{max} = 0.001. Positional coordinates are included in Table 2. The atomic scattering factors for Os(III) and Na⁺ were taken from refs 19 and 20, respectively.

Equilibrium and Kinetic Studies. The constant for the equilibrium [Os(CN)₅NO]²⁻ + 2OH⁻ ⇌ [Os(CN)₅NO₂]⁴⁻ + H₂O was determined spectrophotometrically at 25.0 ± 0.2 °C in H₂O, I = 1.0 M (NaCl).

Table 2. Final Positional and Isotropical Parameters for Na₂[Os(CN)₅NO]·2H₂O^a

atom	x	y	z	B _{iso} , ^b Å ²
Os	0.4986(1)	0.2804(0)	0.5000(0)	1.35(1)
N(4)	0.733(1)	0.3613(6)	0.5000(0)	1.8(2)
O(1)	0.891(1)	0.4070(7)	0.5000(0)	4.7(3)
C(1)	0.235(2)	0.1803(9)	0.5000(0)	2.6(3)
N(1)	0.091(2)	0.1222(8)	0.5000(0)	3.8(3)
C(2)	0.607(1)	0.1761(5)	0.5926(4)	2.0(2)
N(2)	0.663(1)	0.1163(5)	0.6428(3)	3.3(2)
C(3)	0.339(1)	0.3672(5)	0.4066(4)	2.2(2)
N(3)	0.248(1)	0.4108(5)	0.3546(3)	3.5(2)
Na(1)	0.5000(0)	0.0000(0)	0.2448(2)	2.6(1)
Na(2)	0.0000(0)	0.0000(0)	0.3755(3)	3.0(1)
Ow	0.174(1)	0.1250(4)	0.2671(3)	4.4(2)

^a In this table and those subsequent, estimated standard deviations in the least significant figure are given in parentheses. N(4) and O(1) correspond to the nitrosyl ligand; numbers 1–3 in C and N relate to axial (1) and equatorial (2, 3) cyanide ligands. Ow relates to O in water. ^b The isotropic equivalent displacement parameter is defined as (4/3)[a²B(1,1) + b²B(2,2) + c²B(3,3) + ab(cos γ)B(1,2) + ac(cos β)B(1,3) + bc(cos α)B(2,3)].

Eight solutions containing a fixed amount of [Os(CN)₅NO]²⁻, 4.85 × 10⁻⁴ M, and different concentrations of NaOH (range 0.01–1 M) were prepared; all of them contained a fixed concentration of nitrite ion (ca. 0.01 M) in order to minimize the aquation reaction of [Os(CN)₅NO₂]⁴⁻. After attaining equilibrium (ca. 48 h), the spectra were recorded between 250 and 440 nm. The data were treated according to the NIPALS procedure;²¹ in the latter, the absorbance matrix (the absorbance as a function of wavelength and pH) is decomposed into a product of target and projection matrices. Using a suitable chemical model, these matrices can be transformed into the concentration profile and the spectra of all the species involved. By using the A + 2OH⁻ ⇌ B scheme and employing standard non linear least squares fitting methods,²² the equilibrium constant can be calculated. By performing the global analysis with the raw spectra, a value of K_{eq} = 42 ± 1 M⁻² was obtained, but the resulting spectra of A and B were disturbed by the presence of free nitrite. In order to improve the assignment of the true species involved in the equilibria, the spectrum of a solution of free nitrite at the same concentration as used in the experiment was subtracted to the set of spectra. Thus, a new calculation was performed and the same value of K_{eq} was obtained; in addition, consistent values were now obtained for the spectra of A ([Os(CN)₅NO]²⁻) and B ([Os(CN)₅NO₂]⁴⁻). For the latter species, calculated λ_{max} and ε values were 330 nm and 4500 M⁻¹ cm⁻¹, respectively, in agreement with experimental values obtained when the equilibrium attained a high degree of conversion, at high [OH⁻] concentration.

The rate of [OH⁻] addition to [Os(CN)₅NO]²⁻ was measured by mixing a solution of [Os(CN)₅NO]²⁻ (ca. 1 × 10⁻⁴ M) containing free NO₂⁻ (0.01 M) with a solution of NaOH (range 0.2–1 M; I = 1.0 M). The changes in absorbance with time were recorded between 250 and 440 nm. Absorbance data at the maximum of the product, 330 nm, were fitted to an exponential model using non linear least squares regressions, with the preexponential and the exponential factors as adjusting parameters. From measurements at different temperatures, the activation parameters were calculated by Eyring plots and least squares treatment of the data.

The reaction of [Os(CN)₅NO]²⁻ with SH⁻ was followed by measuring the increase of absorption of the initially formed product at 438 nm, with [Os(CN)₅NO]²⁻ = 1 × 10⁻⁴ M and [SH⁻] = 1.33 × 10⁻¹ M (25.0 °C; pH = 12.0; I = 1 M NaCl). The reaction of [Ru(CN)₅NO]²⁻ (ca. 1 × 10⁻⁴ M, prepared according to the technique described above for the osmium complex) with SH⁻ (1.23 × 10⁻³ M) was studied in similar conditions, by following the increase of the absorption at the corresponding maximum, λ = 430 nm. The data were treated under pseudo first order conditions, in the same way as done for the reaction with OH⁻. Independent stoichiometric experiments were performed for the reaction of [Os(CN)₅NO]²⁻ with each of the nucleophilic

- (16) Krause, R. A.; Violette, C. *Inorg. Chim. Acta* **1986**, *113*, 161.
 (17) Sheldrick, G. M. SHELX 86, Program for Solution of Crystal Structure. University of Göttingen, Germany, 1985.
 (18) Sheldrick, G. M. SHELX 76, Program for Crystal Structure Determination. University of Cambridge, U.K., 1976.
 (19) Cromer, D. T.; Waber, J. T. In *International Tables for X-ray Crystallography*; Kynoch Press: Birmingham: U.K., 1974; Vol IV.
 (20) Doyle, P. A.; Turner, P. S. *Acta Crystallogr. Sect. A: Cryst. Phys. Diffraction, Theor. Gen. Crystallogr.* **1968**, *A24*, 390.

- (21) Malinowski, E. R. *Anal. Chem.* **1977**, *49*, 606, 612.
 (22) Kubista, M.; Sjöback, R.; Albinsson, B. *Anal. Chem.* **1993**, *65*, 994.

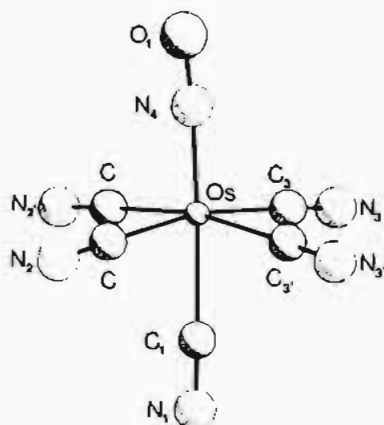


Figure 1. Geometry of the $\text{Os}(\text{CN})_5\text{NO}_2^-$ anion.

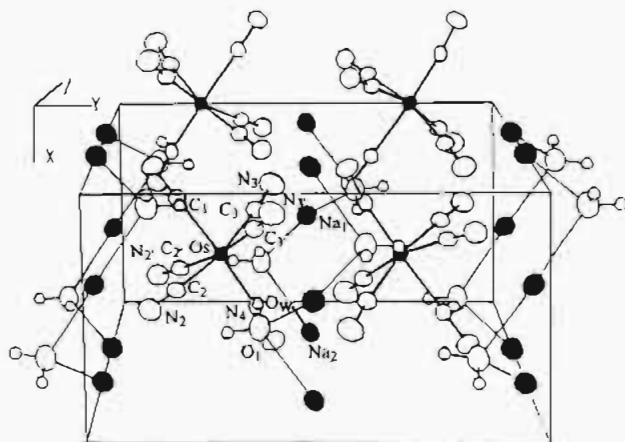


Figure 2. Drawing of the unit cell of $\text{Na}_2[\text{Os}(\text{CN})_5\text{NO}] \cdot 2\text{H}_2\text{O}$ showing the atom labeling scheme. Small and large shaded circles are osmium and sodium atoms, respectively. Hydrogen atoms (small open circles), although not found in the present work, are included for a better identification of Ow atoms, following the structure of the ruthenium analogue (cf. ref 6).

species: OH^- (0.9 M), SH^- (0.1 M), N_2H_4 (0.1 M) in the presence of 1 M pyrazine (pz), at 60 °C. The absorption of the final, stable product, $[\text{Os}(\text{CN})_5\text{pz}]^{3-}$ ($\lambda_{\text{max}} = 386 \text{ nm}$; $\epsilon = 6300 \text{ M}^{-1} \text{ cm}^{-1}$),¹⁵ was checked after the completion of each reaction. The rates of increase of absorption at the maxima of the $[\text{M}(\text{CN})_5\text{pz}]^{3-}$ ions were used for an estimation of the rate of the reaction of N_2H_4 with $[\text{M}(\text{CN})_5\text{NO}]^{2-}$ ($\text{M} = \text{Fe}, \text{Ru}, \text{Os}$).

Results

The structure consists of packed layers of anions, linked by sodium cations and water molecules, as was described elsewhere.⁶ Figures 1 and 2 show the geometry of the anion and the description of the unit cell, respectively. Bond lengths and angles within the anion are displayed in Table 3. The coordination polyhedron around osmium is a slightly distorted octahedron; the distortion trends have been analyzed previously and are quantitatively very similar in the three isostructural (Fe, Ru, Os) compounds.^{6,23} One of the most relevant features is the displacement of the osmium atom out of the plane of the cis-C and toward the NO group, by 0.1906(4) Å.

The results in Table 3 show that an almost linear Os(II)-N-O bonding scheme is present, typical for NO^+ binding to an octahedral low-spin d^6 metal center.¹⁰ The Os-N and N-O distances are indicative of a multiple character of the Os-N-O bond.

Table 3. Selected Bond Lengths (Å) and Bond Angles (deg) within the Pentacyanonitrosylate(II) Anion

Lengths			
Os-C(1)	2.06(1)	C(1)-N(1)	1.15(1)
Os-C(2)	2.051(6)	C(2)-N(2)	1.131(8)
Os-C(3)	2.074(6)	C(3)-N(3)	1.134(8)
Os-N(4)	1.774(8)	N(4)-O(1)	1.14(1)
Angles			
Os-N(4)-O(1)	175.5(7)	C(2)-Os-C(2')	91.2(2)
Os-C(1)-N(1)	178.3(9)	C(2)-Os-C(3)	169.3(2)
Os-C(2)-N(2)	178.0(6)	C(2)-Os-C(3')	87.9(2)
Os-C(3)-N(3)	177.3(6)	C(3)-Os-C(3')	90.9(2)
C(1)-Os-N(4)	177.4(4)	N(4)-Os-C(2)	93.5(2)
C(1)-Os-C(2)	84.7(3)	N(4)-Os-C(3)	97.2(2)
C(1)-Os-C(3)	84.5(3)		

Table 4. Selected Wavenumbers (cm^{-1}) and Assignments in the Infrared Spectra of $\text{Na}_2[\text{M}(\text{CN})_5\text{NO}] \cdot 2\text{H}_2\text{O}$ ($\text{M} = \text{Fe}, \text{Ru}, \text{Os}$)

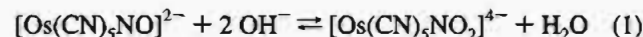
Fe ^a	Ru ^b	Os ^c	assignments ^a	intens
3870	3847	3791	$2\nu(\text{NO})$	m
3267	3633	3637	$\nu_3(\text{OH})$	m
3546	3551	3550	$\nu_1(\text{OH})$	m
2173	2184.0	2183	$\nu(\text{CN}) A_1(\text{ax})$	m
2160	2173.5	2170	$\nu(\text{CN}) A_1(\text{eq})$	m
2156	2165.5	2160	$\nu(\text{CN}) B_1(\text{eq})$	m
2143	2151.0	2145	$\nu(\text{CN}) E(\text{eq})$	s
1945	1926.0	1897	$\nu(\text{NO})$	s
1624	1623	1625		sh
1618	1617	1617	$\delta(\text{HOH})$	m
1612	1612	1610		sh
666.5	645	638	$\nu(\text{MNO}) E$	m
656.8	585	586	$\nu(\text{MN}) A_1$	m
519	512	510	$L(\text{H}_2\text{O})$	m, br
468	460	476	$\nu(\text{MC}) A_1(\text{ax})$	w
433	422	444	$\nu(\text{MC}) E(\text{eq})$	sh
424	410	420		
417	400	407	$\nu^b(\text{MCN}) E$	s
342	350	340	$L(\text{H}_2\text{O})$	m, br
321.5	310	314	$\nu^a(\text{MCN}) E$	m

^a Data and assignments from ref 24. ^b Data from ref 6. ^c This work.

The lengths of the trans- and cis-Os-C bonds are equal within experimental error (mean value 2.06(1) Å) and the same is observed with the trans- and cis-C-N bonds (mean value 1.14(1) Å). The picture is the same as that of the iron compound²³ and quite similar to the ruthenium one too; only a minor shortening of the trans-C-N bond was observed in the latter.⁶

The sodium atoms are surrounded by O- and N-atoms (from water and cyanide, respectively), arranged in slightly distorted octahedra. Although H atoms were not found, we infer that the hydrogen bonding scheme is similar to the one described for the iron and ruthenium complexes;⁶ this is supported by the similar band structure and energies for the O-H stretchings and $\delta(\text{HOH})$ bendings, as shown in Table 4, which also contains the results for other vibrations. The assignments are straightforward, by comparison with the ruthenium⁶ and iron²⁴ compounds. The UV-visible spectrum is shown in Figure 3; the results and proposed assignments are displayed in Table 5.

As for related nitro-nitrosyl complex pairs with other metal centers, the optical spectra are pH dependent, due to an acid-base interconversion between the two forms,²⁵ eq 1.



By adding OH^- at concentrations higher than 1 M, the spectrum of $[\text{Os}(\text{CN})_5\text{NO}]^{2-}$ (Figure 3) changes to the spectrum shown in Figure 4, corresponding to $[\text{Os}(\text{CN})_5\text{NO}_2]^{4-}$. The

(23) Bottomley, F.; White, P. S. *Acta Crystallogr.* 1979, B35, 2193.

(24) Khanna, R. K.; Brown, C. W.; Jones, L. H. *Inorg. Chem.* 1969, 8, 2195.

(25) Bottomley, F. *Acc. Chem. Res.* 1978, 11, 158.

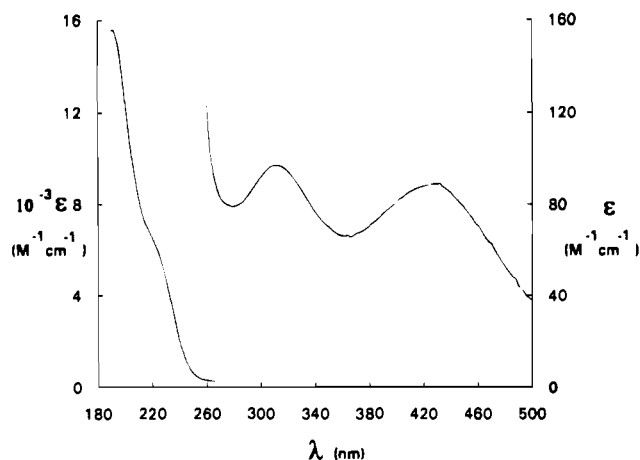


Figure 3. UV-visible spectrum of $\text{Na}_2[\text{Os}(\text{CN})_5\text{NO}] \cdot 2\text{H}_2\text{O}$ in aqueous solution.

Table 5. Electronic Spectral Data and Assignments in the $[\text{M}(\text{CN})_5\text{NO}]^{2-}$ Ions ($\text{M} = \text{Fe}, \text{Ru}, \text{Os}$)

band assigns ^a	ν, cm^{-1} ($\epsilon_{\text{max}}, \text{M}^{-1} \text{cm}^{-1}$)		
	Fe ^a	Ru ^b	Os ^c
$2b_2(xy) \rightarrow 7e$	20 080 (8)	22 988 (26)	23 420 (89)
$6e(xz, yz) \rightarrow 7e$	25 380 (25)	28 985 (39)	31 850 (97)
$2b_2(xy) \rightarrow 3b_1(x^2 - y^2)$	30 300 (40)		
$6e(xz, yz) \rightarrow 5a_1(z^2)$	37 800 (900)	39 215 (1550)	45 450 (6500)
$6e(xz, yz) \rightarrow 3b_1(x^2 - y^2)$	42 000 (700)		
$2b_2(xy) \rightarrow 8e$	50 000 (24 000)	50 000 (9400)	52 080 (15 600)

^a Data and assignments from ref 34. ^b Data from ref 6. ^c This work.

transformation is reversible upon further acidification. In the range $[\text{OH}^-] = 0.1\text{--}1 \text{ M}$, both forms are present and the equilibrium constant can be obtained, as described in the Experimental Section. In Table 6 are shown the results of this experiment and those of similar measurements on Fe and Ru complexes from earlier reports.

In the reaction of the $[\text{Os}(\text{CN})_5\text{NO}]^{2-}$ with OH^- , the k_{obs} values (s^{-1}) increased with the concentration of OH^- , but a rigorous first-order law in each of the reactants was not obeyed in the complete concentration range, as shown in Figure 5. The data can be adjusted to the following rate law, by using non-linear least squares techniques:

$$k_{\text{obs}} = a[\text{OH}^-] + \frac{b}{[\text{OH}^-]}$$

$a = 1.34 \times 10^{-4}$ and $b = 3.9 \times 10^{-6}$.

In the reactions of the $[\text{Os}(\text{CN})_5\text{NO}]^{2-}$ and $[\text{Ru}(\text{CN})_5\text{NO}]^{2-}$ ions with SH^- , the initial increase is followed by a decrease in absorption. From the increasing absorption traces, k_{obs} values (s^{-1}) were obtained, but the rate law was not first order in $[\text{SH}^-]$.

The $[\text{Os}(\text{CN})_5\text{NO}]^{2-}$ ion reacts with hydrazine through the formation of N_2O and a quantitative formation of the $[\text{Os}(\text{CN})_5\text{H}_2\text{O}]^{3-}$ ion. A detailed stoichiometric and kinetic study of this reaction, as well as those of the related processes with the iron and ruthenium species is underway;²⁹ our preliminary results show that the relative rates of N_2H_4 addition toward the three $[\text{M}(\text{CN})_5\text{NO}]^{2-}$ ions are the same as found with OH^- and

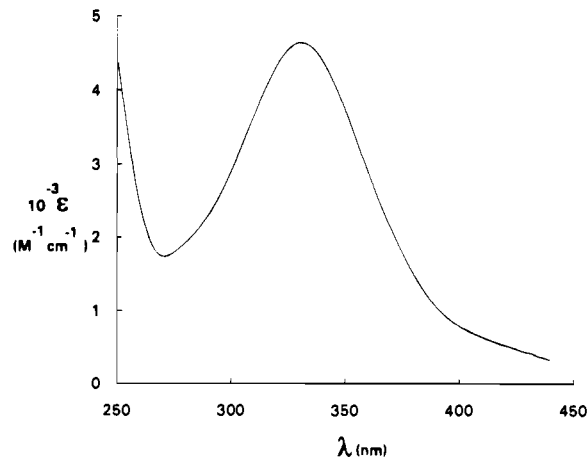


Figure 4. UV-visible spectrum of $\text{Os}(\text{CN})_5\text{NO}_2^{4-}$ in aqueous solution.

SH^- . Also, for a given metal, the rates of N_2H_4 and OH^- addition are of the same order of magnitude.

Discussion

The key feature in analyzing the structural, spectroscopic and reactivity results is related to the intrinsic high π -donor capability of $\text{Os}(\text{II})$,³ which manifests strongly when π -acceptor ligands such as cyanide and nitrosyl are present.

(a) **Structural Data and IR Spectroscopy.** The N–O and Os–N lengths found for some octahedral, linear osmium nitrosyl compounds span the range 1.14–1.21 and 1.68–1.77 Å, respectively.³⁰ They show a sensitive dependence on the nature of the “spectator” ligands but their sum remains approximately constant in the series (ca. 2.90 Å). The values for the presently reported complex (1.14(1), 1.774(8) Å) stand in the lower and higher limits of the published data for the N–O and Os–N bond lengths, respectively. In the presence of competitive π -acceptor ligands such as cyanides, a relatively lower π -back bonding interaction is established between $\text{Os}(\text{II})$ and the NO^+ ligand. On the other hand, with a π -donor spectator ligand such as fluoride, the N–O and Os–N bond lengths are 1.18(1) and 1.707(9) Å, respectively, as found in $[\text{OsF}_5\text{NO}]^{2-}$.³⁰

For the three $[\text{M}(\text{CN})_5\text{NO}]^{2-}$ species ($\text{M} = \text{Fe}, \text{Ru}, \text{Os}$), the N–O length is insensitive to changes in bonding: 1.124 (7) Å (Fe);²³ 1.130 (4) Å (Ru);⁶ the expected increase in length for the osmium derivative (associated with stronger back-donation) is obscured by the experimental uncertainties. Better evidence on the back bonding tendencies is given by $\nu(\text{NO})$ (see Table 4), which decreases in the trend predicted by the higher overlapping ability and closer energy of 5d toward the $\pi^*(\text{NO})$ orbital, compared to that from 4d and 3d orbitals.⁶ We are assuming that $\nu(\text{NO})$ values depend mainly on the π -component of the metal– NO^+ bond, since NO^+ is a poor σ donor.³¹

The M–N, as well as the M–C and C–N lengths are very similar for the ruthenium and osmium pentacyanonitrosyl complexes. The stronger σ - and π -interactions for $\text{Os}(\text{II})$ vs $\text{Ru}(\text{II})$ toward NO^+ and CN^- probably compensate for the slight differences in atomic, covalent and ionic radii, which are higher for Os by 0.01–0.02 Å.³² The similar values for $\nu(\text{MN})$ and $\nu(\text{MC})$ for both ruthenium and osmium compounds are in agreement with this proposal (the greater mass of Os should be compensated by a higher force constant for the stretching vibration).

(25) Chevalier, A. A.; Gentil, L. A.; Olabe, J. A. *J. Chem. Soc., Dalton Trans.* **1991**, 1959.

(26) (a) Swinehart, J. H.; Rock, P. A. *Inorg. Chem.* **1966**, *5*, 573. (b) Masek, J.; Wendt, H. *Inorg. Chim. Acta* **1969**, *3*, 455.

(27) Rock, P. A.; Swinehart, J. H. *Inorg. Chem.* **1966**, *5*, 1078.

(28) Chevalier, A. A.; Amorebieta, V.; Gentil, L. A.; Olabe, J. A. Work in progress.

(29) Sveklov, A. A.; Sinityn, N. M. *Russ. J. Inorg. Chem.* **1986**, *31*, 1667.

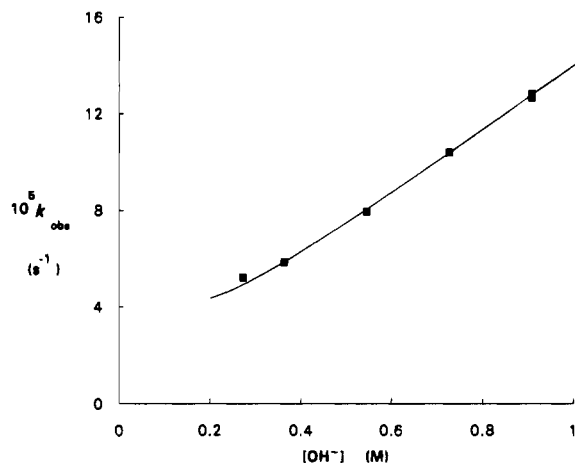
(30) (a) Fenske, R. F.; DeKock, R. L. *Inorg. Chem.* **1972**, *11*, 437. (b) Bottomley, F.; Grein, F. *J. Chem. Soc., Dalton Trans.* **1980**, 1359.

(31) (a) Table of Periodic Properties of the Elements. Sargent-Welch Scientific Co., 1968. (b) Ball, M. C.; Norbury, A. H. *Physical Data for Inorganic Chemists*; Longman: London, 1974.

Table 6. Equilibrium Constants for the OH⁻ Addition Reaction, Nitrosyl-Stretching Wavenumbers, Nucleophilic Rate Constants, k_N (N = OH⁻, SH⁻) and Activation Parameters for the Reactions of the [M(CN)₅NO]²⁻ Ions (M = Fe, Ru, Os)

complex	K_{eq} , M ⁻²	$\nu(\text{NO})$, cm ⁻¹	k_{OH^-} , M ⁻¹ s ⁻¹ ^a	$\Delta H_{\text{OH}^-}^\ddagger$, kJ/mol	$\Delta S_{\text{OH}^-}^\ddagger$, J/K mol	k_{SH^-} , M ⁻¹ s ⁻¹ ^a
[Os(CN) ₅ NO] ²⁻	4.2×10^1	1897	1.37×10^{-4}	80	-49	~0.13
[Ru(CN) ₅ NO] ²⁻	4.4×10^6	1926 ^b	0.95 ^c	57 ^c	-54 ^c	~160
[Fe(CN) ₅ NO] ²⁻	1.5×10^5	1945 ^d	0.55 ^e	53 ^e	-73 ^e	170 ^f

^a $T = 25.0$ °C; $I = 1$ M (NaCl). ^b From ref 6. ^c From ref 26. ^d From ref 24. ^e From ref 27. ^f From ref 28.

**Figure 5.** Plot of the pseudo-first-order rate constant for the formation of Os(CN)₅NO₂⁴⁻, k_{obs} (s⁻¹), (addition of OH⁻ to Os(CN)₅NO²⁻), against the concentration of OH⁻ ($T = 25$ °C, $I = 1$ M). The continuous trace is a fitting of the experimental data according to the proposed rate law (see text).

The constancy in C–N bond length, as well as the absence of a definite trend in the $\nu(\text{CN})$ values for the three [M(CN)₅NO]²⁻ species, do not warrant a detailed discussion on the bonding properties of cyanide; to be sure, the cyanide behavior appears to be more complex than NO⁺, because σ -donor, π -donor and π -acceptor properties should all be important in the interaction with the three metals.³¹

The strong intramolecular, electron-withdrawing effect of the NO⁺ ligand is mainly reflected in the high value of $\nu(\text{CN})$, 2145 cm⁻¹, which is significantly higher than that found in [Os(CN)₆]⁴⁻, 2040 cm⁻¹.³³ The same trend was observed with the ruthenium compounds.⁶ The Os–C distances, however, do not change significantly in both compounds.

(b) Electronic Spectra and Assignments. In the electronic spectrum (Figure 3) the two lower energy bands (assigned to Os(II)→ $\pi^*(\text{NO})$ transitions) shift to higher wavenumbers if compared to similar bands measured for ruthenium⁶ and iron³⁴ derivatives (Table 5). The shift is higher for the 6e→7e transition, as it involves a ground state which is strongly stabilized through the π -interaction, thus raising the energy of the $\pi^*(\text{NO})$ level. On the other hand, the energy of the 2b₂→7e transition is only slightly increased in the osmium compound, because the 2b₂ level has a nearly nonbonding character with respect to the nitrosyl interaction. The band at 192 nm can be

assigned to the 2b₂→8e (Os(II)→ $\pi^*(\text{CN})$) transition, and the shoulder (220 nm) to a “d–d” transition, shifted to higher energy with respect to Ru and Fe, in agreement with the stronger ligand field in osmium.³⁵

(c) Equilibrium and Kinetic Studies. (i) **Reaction of [Os(CN)₅NO]²⁻ with OH⁻.** The reactions of OH⁻ with coordinated nitrosyl complexes have been widely studied and can be considered as a prototype model for comparing the electrophilic reactivity of the latter species.²⁵ The stoichiometry of the addition reaction of OH⁻ to [Os(CN)₅NO]²⁻ (reaction 1) is equivalent to the one found for the ruthenium and iron analogues,^{26,27} as well as for other d⁶ low-spin complexes.²⁵ The band maximum and molar absorbance of the product are consistent with a MLCT transition from $d\pi(\text{Os})$ to the antibonding orbital mainly localized at the N-bound nitrite-ligand.

Table 6 shows that the value of K_{eq} for the addition reaction of the osmium complex is significantly lower than those found for the iron- and ruthenium-complexes. Interestingly, the same is found for the kinetic rate constant for the formation of the nitro-complex, k_{OH^-} . A linear correlation is found by plotting $\ln(k_{\text{OH}^-})$ against $\ln(K_{eq})$ with a slope of 0.7 ($r = 0.999$). The equilibrium constants have been measured for a wide range of complexes, but k_{OH^-} values have been only obtained for the pentacyanonitrosyl ions;¹² the correlation suggests that either parameter can be used as an indicator of the electrophilic reactivity of coordinated nitrosyl. Through the analysis of K_{eq} and the corresponding $\nu(\text{NO})$ values, it was found that the higher electrophilic reactivities were associated with high values of both K_{eq} and $\nu(\text{NO})$, as in the case of the [IrCl₅NO]⁻ ion ($K = 6 \times 10^{29}$ M⁻², $\nu = 2006$ cm⁻¹);³⁶ a lower limit was found for the [RuCl(V)₂NO]⁴⁻ ion (V = violurate anion), ($K_{eq} = 5 \times 10^{-2}$ M⁻², $\nu = 1885$ cm⁻¹).³⁷ From the author's descriptions,^{36,37} we infer that the rates of formation of the corresponding nitro-complexes are very rapid and slow, respectively, in a qualitative agreement with the k_{OH^-} vs K_{eq} correlation.

The correlation of K_{eq} vs $\nu(\text{NO})$ seems to hold reasonably well when a series of complexes containing the same metal center is analyzed; thus, in the series [RuCl(V)₂NO]⁴⁻, [Ru(CN)₅NO]²⁻, [RuCl(bpy)₂NO]²⁺³⁸ and [Ru(trpy)(bpy)NO]³⁺³⁹ the K_{eq} (and ν) values increase as follows: 5×10^{-2} (1885); 4.4×10^6 (1926); 1.6×10^9 (1927); 2.1×10^{23} (1952). It can be seen that the trends are related to the nature of the auxiliary ligands; if the latter compete strongly for the π -electron density with NO⁺ (as in the case of polypyridinic ligands), a lower electron density is placed on the N-atom of coordinated nitrosyl, or, in an alternative formulation, on the $\pi^*(\text{NO})$ orbital. On the other hand, π -donor ligands such as chloride, act in the opposite sense.

For osmium nitrosyl-complexes, only data for [Os(CN)₅NO]²⁻ and for [Os(trpy)(bpy)NO]³⁺ ($K_{eq} = 7.0 \times 10^{10}$ M⁻², $\nu = 1904$ cm⁻¹)³⁹ are available. The lower values in the pentacyanoni-

(33) Gentil, L. A.; Navaza, A.; Olabe, J. A.; Rigotti, G. E. *Inorg. Chim. Acta* **1991**, *179*, 89.

(34) Manoharan, P. T.; Gray, H. B. *Inorg. Chem.* **1966**, *5*, 823.

(35) The stronger ligand field in the Os compound can be attributed (in a molecular orbital language) both to a lower energy of the bonding and a higher energy of the antibonding d orbitals on the metal. The stabilization of the bonding orbitals relates to the stronger π -interactions in osmium, as already discussed. On the other hand, the destabilization of the antibonding σ -orbitals relates to the strength of the σ -interaction, which raises the energy of the σ^* orbital on the metal. Our independent kinetic results on the dissociation of N₂H₄ (a “ σ -only” ligand) from the [M(CN)₅N₂H₄]³⁻ ions (M = Fe, Ru, Os), show that the rate is significantly slower in the osmium compound, suggesting a stronger σ -interaction. We can reasonably expect a similar trend for the other ligands as well (such as cyanide or nitrosyl).

(36) (a) Bottomley, F.; Brooks, W. V. F.; Clarkson, S. G.; Tong, S. B. *J. Chem. Soc., Chem. Commun.* **1973**, 919. (b) Bottomley, F.; Clarkson, S. G.; Tong, S. B. *J. Chem. Soc., Dalton Trans.* **1974**, 2344.

(37) Sueur, S.; Bremard, C.; Nowogrocki, G. J. *Inorg. Nucl. Chem.* **1976**, *38*, 2037.

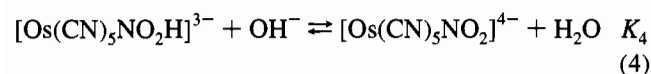
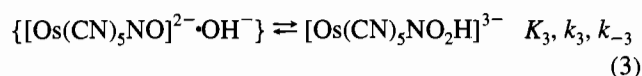
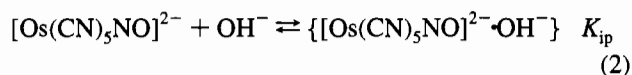
(38) Godwin, J. B.; Meyer, T. J. *Inorg. Chem.* **1971**, *10*, 2150.

(39) Pipes, D. W.; Meyer, T. J. *Inorg. Chem.* **1984**, *23*, 2466.

trotyl complex are in agreement with the previously discussed trends for the Ru(II) complexes. On the other hand, for the same ligand environment, Os(II) complexes show lower values than Ru(II) ones, and this is consistent with the well-known stronger π -donor ability of Os(II) compared to Ru(II).³

Table 6 shows that the K_{eq} value for the $[\text{Fe}(\text{CN})_5\text{NO}]^{2-}$ ion is lower than the one for the ruthenium complex, in contrast to the trends in $\nu(\text{NO})$. As proposed previously, other factors in addition to the back-bonding abilities could influence the nucleophilic trends, namely the polarizability of the reactants.²⁶ Thus, the higher polarizability of $[\text{Ru}(\text{CN})_5\text{NO}]^{2-}$ could compensate for the unfavorable electronic density at its $\pi^*(\text{NO})$ level, as measured by $\nu(\text{NO})$. On the other hand, for ruthenium and osmium nitrosyl complexes, which have similar radii, the relative nucleophilic rates appear to be clearly determined by the back-bonding abilities, as shown above.

In order to account for the rate law for the formation of $[\text{Os}(\text{CN})_5\text{NO}_2]^{4-}$, we propose the following mechanistic scheme:



This is essentially equal to that previously proposed for the ruthenium²⁶ and iron²⁷ complexes, although with the present inclusion of the rapid, outer-sphere association step (2). Thus, reaction 3 includes the rate determining nucleophilic addition step, k_3 , and is followed by reaction 4, a rapid deprotonation process with a high equilibrium constant.

The predicted rate law (see Appendix) agrees very well with the experimental data

$$k_{\text{obs}} = k_{\text{OH}^-} \left([\text{OH}^-] + \frac{1}{K_{\text{eq}}[\text{OH}^-]} \right)$$

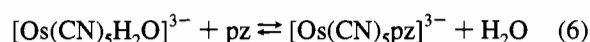
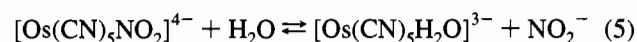
In this interpretation, $k_{\text{OH}^-} = K_{ip}k_3$ and $K_{\text{eq}} = K_{ip}K_3K_4$; with the inclusion of K_{ip} , the proposed scheme can be employed for the reactions of other nitrosyl complexes such as those mentioned previously. However, given the wide range of observed K_{eq} values, the calculations show that K_{ip} values are not significantly influencing K_{eq} .⁴⁰ On the same basis, the trends in the k_{OH^-} values are proposed to be representative of the trends in the nucleophilic rate constant for the elementary step, k_3 .

The rate law simplifies to $k_{\text{obs}} = k_{\text{OH}^-} [\text{OH}^-]$ for sufficiently high OH^- values, as shown in Figure 5; the same would occur for a high value of K_{eq} , and this is the reason for previously observing a simple second-order rate law for the reactions of OH^- with ruthenium and iron-complexes.^{26,27} As a bonus, the experimental rate law gives independently a value of $K_{\text{eq}} = a/b = 35 \text{ M}^{-2}$, which is fairly consistent with the one obtained from the spectroscopic equilibrium measurements, 42 M^{-2} .

Some significance can be given to the activation parameters shown in Table 6. The negative entropies are consistent with the interaction of like charges. On the other hand, the decrease in k_{OH^-} for the osmium complex compared to the ruthenium one appears to be mainly related to the higher value of ΔH^\ddagger . By considering a series of complexes containing nitrosyl and polypyridyl ligands, a linear correlation was found between $E_{1/2}$

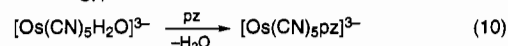
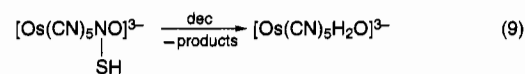
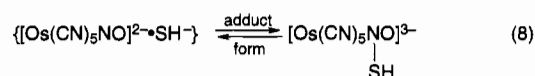
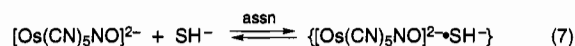
(the potential associated with electrochemical reduction at the nitrosyl ligand) and $\nu(\text{NO})$. By comparing data from the previously mentioned Os and Ru polypyridyl complexes, $\nu(\text{NO})$ is 48 cm^{-1} lower in osmium, corresponding to a shift in $E_{1/2}$ of ca. 0.5 V .³⁹ For the pentacyanonitrosyl complexes of Os and Ru, $\Delta\nu = 29 \text{ cm}^{-1}$ and this should correspond to a difference in the energy of the $\pi^*(\text{NO})$ levels of 0.28 V . The latter number is fairly comparable with the measured difference in ΔH^\ddagger 's, 25 kJ/mol (0.26 V) supporting that in both processes, associated either to the transfer of an electron or the transfer of a OH^- species, the differences are mainly related to the changes in energy of the acceptor orbital.

In the equilibrium and kinetic studies, care was taken to add free nitrite in order to inhibit the aquation reaction of $[\text{Os}(\text{CN})_5\text{NO}_2]^{4-}$. The nitrite ligand can be interchanged by other ligands such as water or pyrazine. This useful synthetic method has been broadly employed in the chemistry of $[\text{M}(\text{CN})_5\text{L}]^{n-}$ systems ($\text{M} = \text{Fe}, \text{Ru}$)⁵⁻⁷ and recently also for the osmium derivatives.¹⁵ By comparison, we infer that the process should involve two well-defined reactions



The quantitative formation of the $[\text{Os}(\text{CN})_5\text{pz}]^{3-}$ ion when the reaction of $[\text{Os}(\text{CN})_5\text{NO}]^{2-}$ with OH^- is carried out in the presence of an excess of pyrazine shows that reactions 2-4 are followed by reactions 5-6.

(ii) **Reactions of $[\text{Os}(\text{CN})_5\text{NO}]^{2-}$ and $[\text{Ru}(\text{CN})_5\text{NO}]^{2-}$ with SH^- .** Both of these reactions follow a similar route to that previously observed with the iron derivative.²⁸ The initial absorption increase has been interpreted as an adduct formation reaction of the nitrosyl complex with the SH^- species, as in reaction 3. The nature of the process(es) associated with the further decay of the adduct absorption is however unclear, probably involving adduct rearrangements and redox transformations.^{41,42} Our present study shows however that, independently of the nature of the latter processes, a quantitative formation of $[\text{Os}(\text{CN})_5\text{pz}]^{3-}$ is also obtained when the reaction is performed in excess of pyrazine, suggesting that the following reaction scheme (eqs 7-10) is operative:



For our present purposes, the kinetic data obtained from the rising absorption traces seems to be adequate for the sake of comparisons. It should be emphasized, however, that we did not find a rigorous first-order rate law in each of the reactants, as proposed for the iron complex.²⁸ In our experiments, the rate law appears to be more complex, suggesting that the formation and decomposition rates of the adduct are occurring in the same time scale. If the observed k values (s^{-1}) are divided by the concentration of SH^- , apparent second-order rate constant

(41) Swinehart, J. H.; *Coord. Chem. Rev.* **1967**, *2*, 385.

(42) (a) Morando, P. J.; Borghi, E. B.; Scheingart, L. M.; Blesa, M. A. *J. Chem. Soc., Dalton Trans.* **1981**, 435. (b) Johnson, M. D.; Wilkins, R. G. *Inorg. Chem.* **1984**, *23*, 231.

values, k_{SH^-} , can be obtained; these values (Table 6) can be considered as representative of the nucleophilic trends of SH^- toward the $[\text{M}(\text{CN})_5\text{NO}]^{2-}$ ions ($\text{M} = \text{Fe}, \text{Ru}, \text{Os}$); the k_{SH^-} values reproduce the trends previously discussed for the OH^- reactions, the osmium complex showing the lowest rate, while the ruthenium and iron complexes react with similar rates. Also, for a given metal, k_{SH^-} is systematically higher than k_{OH^-} , in agreement with the higher polarizability of the sulfur species. The latter numbers support the proposed reaction scheme even in the absence of a clear mechanistic picture of the overall reaction.

(iii) General Mechanistic Picture of Electrophilic Reactions for $[\text{Os}(\text{CN})_5\text{NO}]^{2-}$. The reaction of OH^- , SH^- and other nucleophilic reagents with the pentacyanonitrosyl complexes can be interpreted on the basis of a general mechanistic scheme related to (7)–(9), including the common onset of association (7) and adduct-formation (8) reversible steps and a further adduct-reorganization reaction (9) which, indeed, is dependent on the type of initial nucleophile. The latter process can be an aquation, as well as a nonredox or redox rearrangement, which can proceed in one or several steps. Redox decomposition processes have been observed with thiols and N-coordinating ligands such as amines and NH_2OH .^{11,12} Our experiments with N_2H_4 show that this is also the case, as shown by the detection of N_2O as a product. In all the cases, the $[\text{Os}(\text{CN})_5\text{H}_2\text{O}]^{3-}$ ion appears to be a common product of the adduct decomposition reactions.

Acknowledgment. This work was supported by the Consejo Nacional de Investigaciones Científicas y Técnicas (CONICET) and by the University of Buenos Aires. We thank Dr. E. E. Castellano for the collection of crystallographic data and valuable discussions and Dr. Robert Binstead (Department of Chemistry, University of North Carolina at Chapel Hill) for providing us with a software package for the multicomponent analysis. The aid of Leonardo Slep in the treatment of equilibrium and kinetic data is also gratefully acknowledged. J.A.O. and G.R. are members of the scientific staff at CONICET and CICPBA (Comisión de Investigaciones Científicas de la Provincia de Buenos Aires), respectively.

Supplementary Material Available: Listings of anisotropic thermal parameters (U_{ij} 's) and additional information on intensity data collection (2 pages). Ordering information is given on any current masthead page.

Appendix

By considering the mechanism shown in eq (2–4), the following expression was obtained for the dependence of the concentration of $[\text{Os}(\text{CN})_5\text{NO}^{2-}]$ with time:

$$[\text{Os}(\text{CN})_5\text{NO}^{2-}] = \frac{B}{A} + \frac{(A[\text{Os}(\text{CN})_5\text{NO}^{2-}]_0 - B)}{A} \exp(-At) \quad (11)$$

with

$$A = K_{\text{ip}}k_3[\text{OH}^-] + \frac{k_{-3}}{1 + K_4[\text{OH}^-]}$$

$$B = \frac{k_{-3}[\text{Os}(\text{CN})_5\text{NO}^{2-}]_0}{1 + K_4[\text{OH}^-]}$$

The previous analysis was based on the same grounds as used in ref 27b; in our case, the new feature in the mechanism is the inclusion of the ion-pair species. Equation 11 was obtained after considering the appropriate mass balance relation for the osmium species, eq 12,

$$[\text{Os}(\text{CN})_5\text{NO}^{2-}]_0 =$$

$$[\text{Os}(\text{CN})_5\text{NO}^{2-}] + \{[\text{Os}(\text{CN})_5\text{NO}]^{2-} \cdot \text{OH}^-\} +$$

$$[\text{Os}(\text{CN})_5\text{NO}_2\text{H}^{3-}] + [\text{Os}(\text{CN})_5\text{NO}_2^{4-}] \quad (12)$$

followed by its differentiation and the assumption of a stationary state for the ion-pair species.

If $K_4[\text{OH}^-] \gg 1$ (a situation certainly found in our experimental conditions) we obtain for A and B :

$$A = K_{\text{ip}}k_3 \left([\text{OH}^-] + \frac{1}{K_{\text{eq}}[\text{OH}^-]} \right)$$

$$B = \frac{K_{\text{ip}}k_3[\text{Os}(\text{CN})_5\text{NO}^{2-}]_0}{K_{\text{eq}}[\text{OH}^-]}$$

By assuming that the concentrations of ion-pair and NO_2H bound species are negligible during the reaction, eq 12 simplifies to:

$$[\text{Os}(\text{CN})_5\text{NO}^{2-}] = [\text{Os}(\text{CN})_5\text{NO}^{2-}]_0 - [\text{Os}(\text{CN})_5\text{NO}_2^{4-}] \quad (12')$$

By substitution into eq 11, the latter becomes:

$$[\text{Os}(\text{CN})_5\text{NO}_2^{4-}] =$$

$$[\text{Os}(\text{CN})_5\text{NO}^{2-}] - \frac{B}{A} - \frac{(A[\text{Os}(\text{CN})_5\text{NO}^{2-}]_0 - B)}{A} \exp(-At)$$

Thus, from the observed experimental trace, we obtain

$$k_{\text{obs}} = A = K_{\text{ip}}k_3 \left([\text{OH}^-] + \frac{1}{K_{\text{eq}}[\text{OH}^-]} \right)$$